Supporting Information

Conversion from Self-Assembled Block Copolymer Nanodomains to Carbon Nanostructures with well-defined Morphology

Ya-Sen Sun, Wei-Hua Huang, Jiun-You Liou, Yen-Hsing Lu, Kuo-Chih Shih, Chien-Fu Lin, and Shao-Liang Cheng

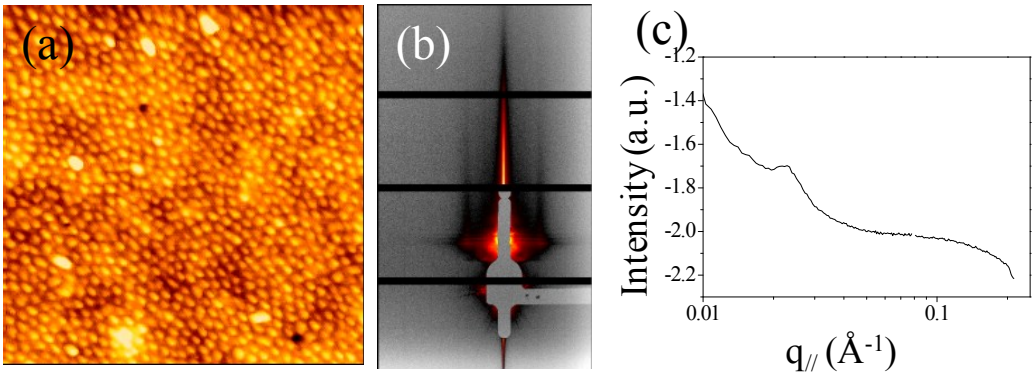

Figure S1 (a) AFM topographic image, (b) GISAXS 2D pattern and (c) 1D in-plane profile with intensity versus $q_{//}$ for disordered micelles within an as-spun $P(S_{50000}2VB_{165000})$ film.

Stabilization of nanodomains by UVIN for pyrolyzed carbonaceous nanostructures

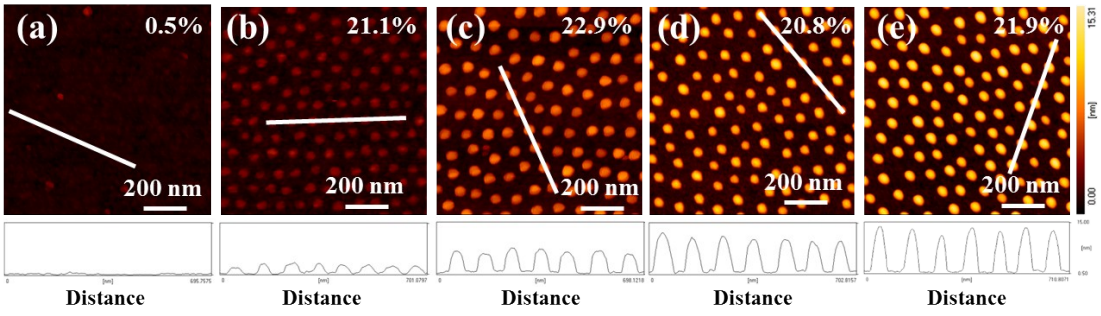

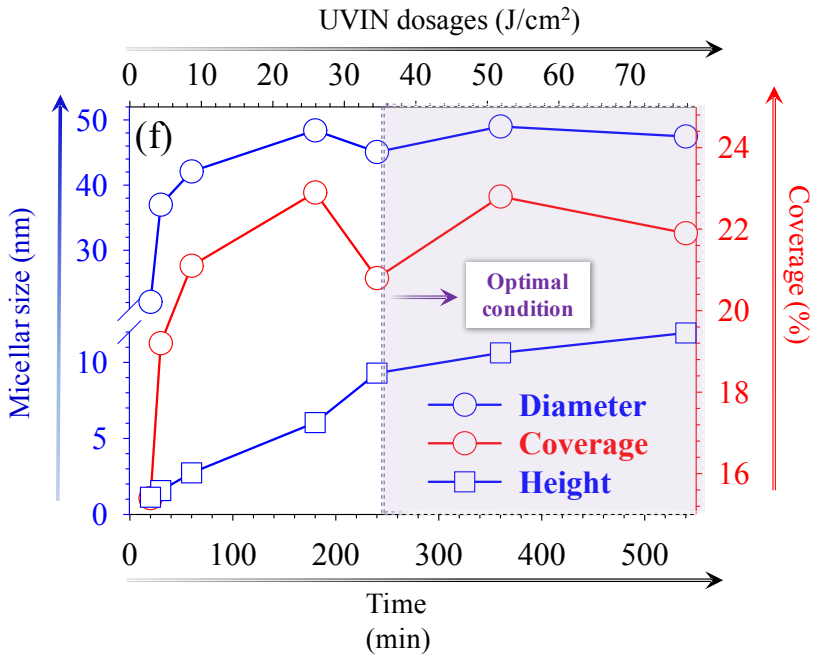

Figure S2 AFM topographic images and corresponding height profiles of granular nanocarbons made from P(S_{48500}2VP_{70000}) S nanodomains after UVIN of (a) 10, (b) 60, (c) 180, (d) 240, and (e) 540 min and subsequent pyrolysis at 430 °C in Ar for 1 hr. White lines represent height profiles as a visual guide. The surface coverage of carbons is shown in the top right. (f) Variations of the height, diameter and coverage of pyrolyzed nanodomains as a function of UVIN dosage and time.

To find an optimal dosage of UVIN for the stabilization of BCP nanodomains, we investigated quantitatively, with an AFM, the structural details of pyrolyzed P(S_{48500}2VP_{70000}) thin films containing one monolayer of *S* nanodomains after exposure to UVIN dosage in a range and subsequent pyrolysis at 430 °C for 1 h under Ar. Since structural details of micelles in the monolayer region have been quantitatively characterized by GISAXS and modeling simulations in our previous work,[1] thus the monolayer serves as a model system for analysis of the impact of cross-linking as a function of UVIN dosage on the shape, size, size distribution, and scattering length density of truncated micelles during pyrolysis processes. The range of UVI dosages was controlled with duration of exposure varied from 10 min (1.44 J/cm²) to 9 h (77.76 J/cm²) under UV light (2.4 mW/cm²) at distance 10 cm from the

sample to the lamp. Thin films containing one monolayer of core-shell truncated micelles with hexagonal lattice order each were prepared by spin coating (at 5000 rpm) from a 0.2 or 0.3 mass % of P(S_{48500}2VP_{70000}) in o-xylene. For the thin films without, or with brief, periods of UVIN, nanodomains were significantly damaged or removed from the substrate through pyrolysis (Figure S2a-c). This result indicates that most materials decomposed to emit volatile hydrocarbons during pyrolysis when the density of cross-linking was small. For specimens with prolonged UVIN treatment of duration more than 3 h, the surface of the pyrolyzed thin films was dominated by small granular carbon nanostructures (Figures S2d-e). Figure S2f shows the variations of the height, diameter and surface coverage of pyrolyzed nanodomains as a function of UVIN dosage (time), obtained from quantitative analysis of the AFM height images (Figure S2a–e). UVIN can be seen to stabilize the dimension of carbon nanostructures during pyrolysis. For brief UVIN, the size of carbon nanostructures increased with increasing UVIN dosage. When the UVIN dosage attained 36 J/cm^{-2} (duration 4 h), both the dimensional variation and the surface coverage of carbon nanostructures attained a plateau, in which region the size of carbon nanostructures remained stable. A dosage 36 J/cm^2 can thus be taken to indicate an optimum UVIN dosage. UVIN has two effects -- cross-linking the polymer chains and increasing the adhesion between nanostructures and an underlying substrate.[2-3] Without UVIN treatment, pyrolysis at 430 ^{o}C led to only a small residue of chaotic carbonaceous species (not shown). Pyrolysis has been demonstrated to cause thermochemical degradation of organic species through chain scission at elevated temperatures.[4] For vinyl polymers, chain scission refers to homolytic bond cleavage at weak points in the polymer chains. The propagation of chain scission eventually produces species of small molar mass and great volatility. As a result, these volatile species flow readily into air, causing severe loss of mass of carbon during pyrolysis. Alternatively, some

volatile species exist in the form of free radicals and thus remain reactive to recombine when pairs of free radicals collide. In the case of pyrolysis of UVIN-treated *S* nanodomains, cross-linking triggered by UV radiation increases the mass density through a decreased free volume within *S* nanodomains.[5] The compact space within the UVIN-treated *S* nanodomains in turn retards the mobility of free radicals generated from chain scission and increases the probability of recombination of free radicals. Both factors diminish the formation of volatile species and thus increase the residue of solid carbonaceous species. Moreover, UVIN-induced cross-linking is accompanied with the protonation of pyridine rings and the formation of network structures within *S* nanodomains. The protonation of pyridine rings is due to transfer of H from cleaved carbon-hydrogen bonds to the nitrogen atom of the pyridine rings.[6] Our XPS results of nitrogen 1s (N 1s) spectra indicate that UNIN causes a shift 2.3 eV of the binding energy of the N 1s electron.[5] This result implies that protonation of pyridine rings would impose a charge imbalance near the pyridinic nitrogen, which increases molecular polarity and in turn produces a strong polar adhesive interaction of UVIN-treated micelles with SiO_x/Si having polar hydroxyl groups, whereas the formation of compact network structures would increase the *effective* areas of contact between the UVIN-treated *S* nanodomains and the underlying substrate, producing enhanced van der Waals forces at the interface between polymer and substrate[2-3]. The UVIN-treated *S* nanodomains were hence immobile during pyrolysis: the array of granular nanocarbon retained a hexagonal packing.

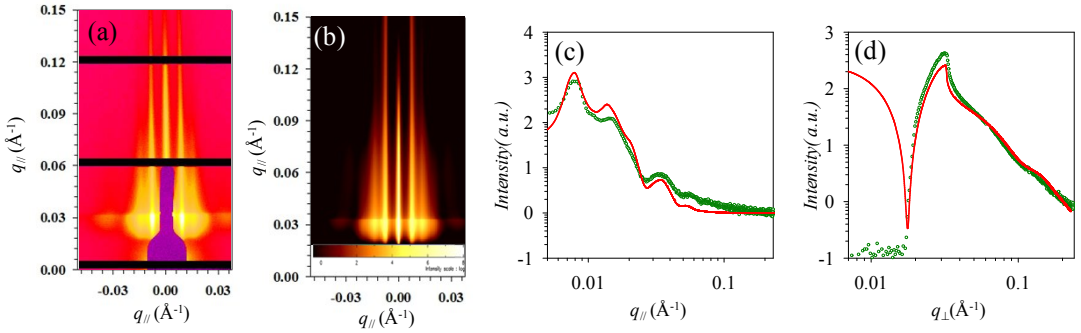

Figure S3 (a) Experimental and (b) simulated GISAXS 2D patterns and 1D in-lane (c) and out-of-plane (d) profiles of granular carbons after S nanodomains were subjected to 4 h of UVIN and then 1h of pyrolysis (simulated parameters: <H> = 7.65 nm, <R> = 23.5 nm, σ_R/<R>=0.123, D=90.5 nm and σ_D/D=0.01).

Figure S3 shows experimental and simulated GISAXS 2D patterns and 1D profiles of granular carbon nanostructures after the *S* nanodomains were subjected to UVIN for 4 h and then pyrolysis for 1 h. The features associated with the form factor of core-shell truncated spheres are absent from Figure S3 for the granular carbon nanostructures. Instead, the experimental GISAXS 2D pattern displays only series of diffraction maxima associated with the structure factor (Figure S3a). This result indicates that pyrolysis of UVIN-treated *S* nanodomains destroyed the core-shell structure but had no influence on the spatial order.

Since GISAXS data reveal complicated scattering profiles or patterns as a result of multiple scattering events in terms of a combination of reflection and refraction effects, GISAXS modeling analyses can only be achieved using the distorted wave Born approximation (DWBA).[7-8] In order to obtain structural details of one monolayer of granular carbon nanostructures, GISAXS 2D images and corresponding 1D profiles were simulated using the IsGISAXS software.[9] This software can provide quantitative analysis for relief nanostructures on a substrate. To model the form factor, we used the model of truncated sphere with hexagonal packing. The interference function of a hexagonal paracrystal of parameter *D* with Gaussian isotropic disorder σ_D/D was used

to describe the spatial arrangement of granular carbon nanostructures on top of SiO_x/Si. For truncated sphere shape, the spatial ordering and structural parameters extracted from the fits include the nearest inter-micelle distance (D), disorder parameter (σ_D/D), the average core radius (<R>) and height (<H>), size distribution of the core radius (σ_R) and scattering length density (SLD). According to the model of truncated spheres with a hexagonal polycrystalline packing, the GISAXS 2D pattern and 1D profile were well reproduced (Figures 3Sb-d).

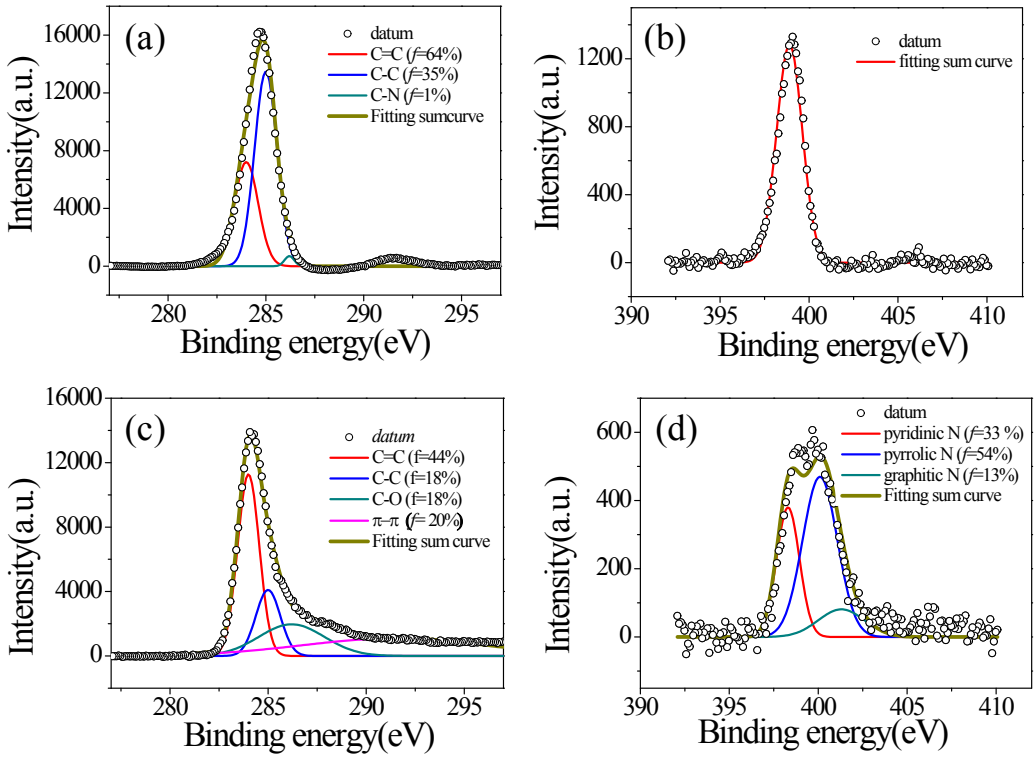

Figure S4 XPS (a, c) C 1s and (b, d) N 1s spectra of a P(S_{50000}2VP_{16500}) film with $C_\perp$ nanodomains (a, b) before and (c, d) after pyrolysis.

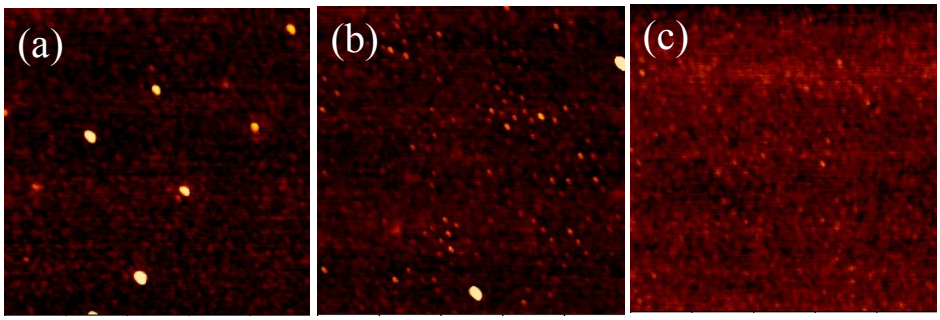

Figure S5 AFM height images of P(S_{50000}2VP_{16500}) thin specimens after UVIN and pyrolysis at various elevated temperatures: (a) 600, (b), 750 and (d) 900 °C

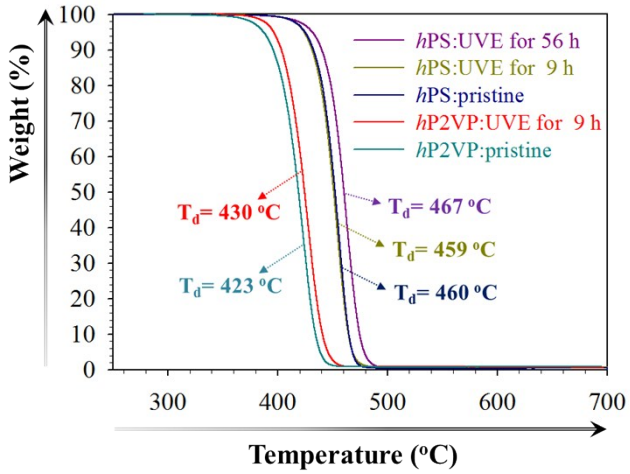

Figure S6 TGA profiles of pristine polymer bulk prepared from *h*PS (blue curve) and *h*P2VP (cyan curve). Then, $h$$PS_{45000}$ and $h$$P2VP_{159000}$ bulk were subjected to UV irradiation in N_2 for 9 h (marked by brown and red curves respectively).

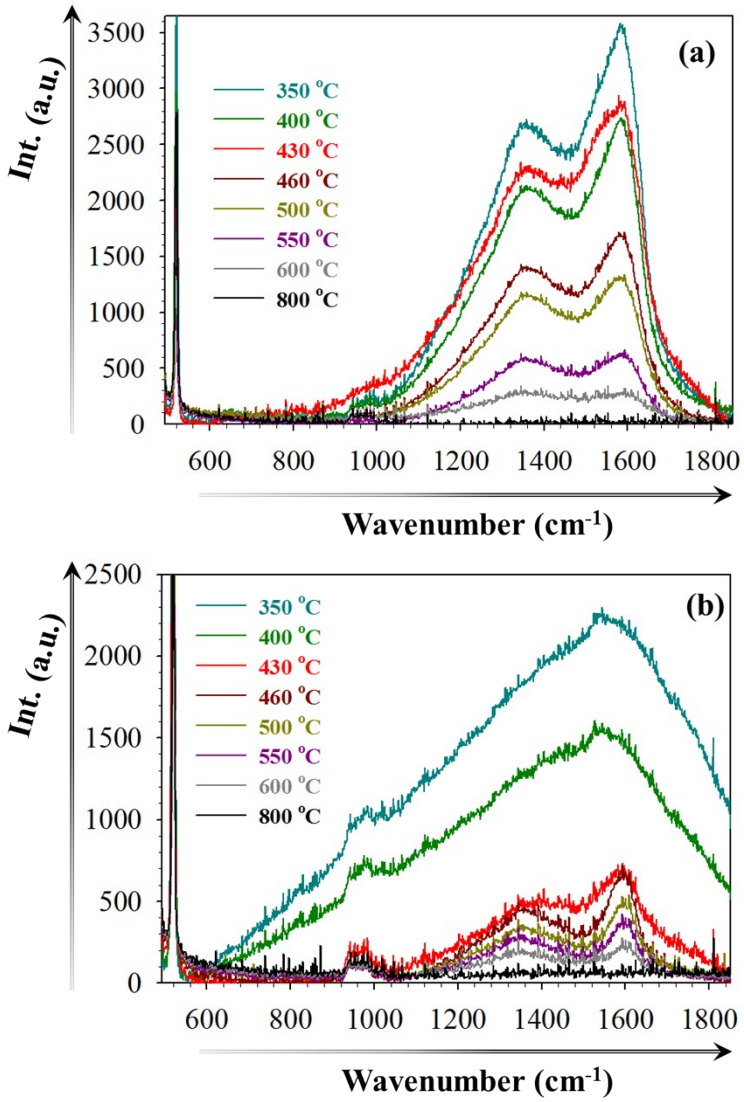

Figure S7 Raman spectra of carbons obtained through pyrolysis of (a) $hP2VP_{159000}$ and (b) hPS_{45000} at elevated temperatures in the range of 350–800 °C.

The in-plane crystal size (L_a) of graphitic carbons was further calculated by analyzing the intensity ratio, I_D/I_G, of the D and G bands based on the Tuinstra–Koenig relationship given as follows.[10]

$$L_a=2.4\times10^{-10}\lambda^4(I_D/I_G)^{-1} \quad (1)$$

where λ is the excitation wavelength (532 nm)

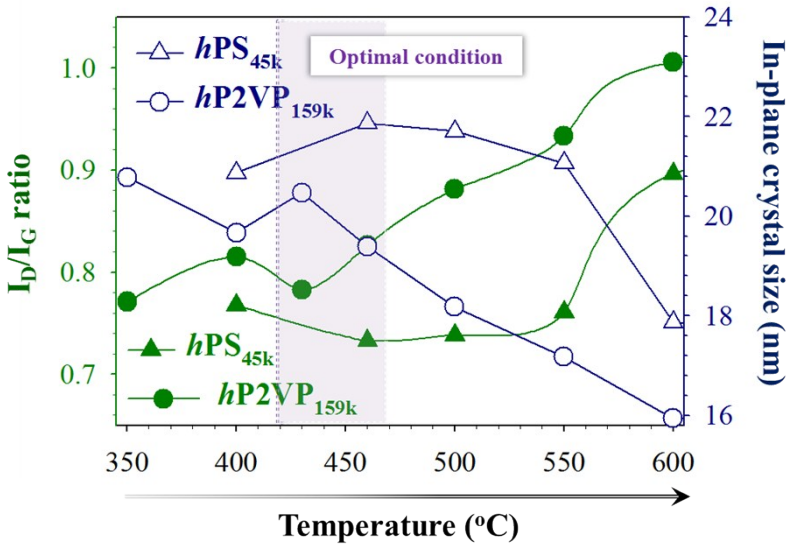

Figure S8 I_D/I_G ratio and in-plane crystal size of hPS$_{45000}$ and hP2VP$_{152000}$ thin films at different carbonized temperature.

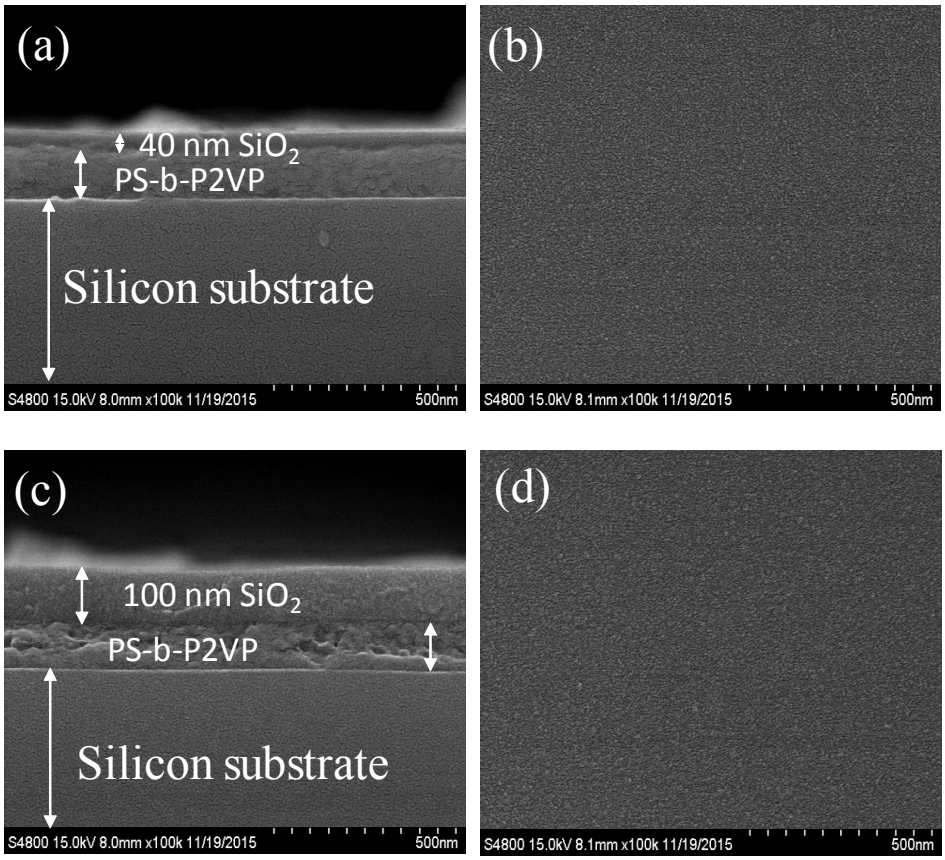

Figure S9 side-view (a, c) and top-view (b, d) SEM images of a pristine P(S_{50000}2VP_{165000}) film with a surface capping SiO_2 layer of 40 or 100 nm.

References

1. J. Y. Liou, Y. S. Sun, *Macromolecules,* 2012. **45**, 1963-1971.
2. M. Yan, B. Harnish, *Adv. Mater.* 2003, **15**, 244-248.
3. Harnish, B.; Robinson, J. T.; Pei, Z.; Ramström, O.; Yan, M. *Chem. Mater.* **2005**, *17*, 4092-4096.
4. M. P. Stevens, *Polymer Chemistry, 2nd edition, Oxford University Press*, 1990, **9**, 296-321.
5. J. Y Liou, Y. S. Sun, *Soft Matter*, 2015, **11**, 7119-7129.
6. A. Elmaci, J. Hacaloglu, *Polymer Degradation and Stability,* 2009, **94**, 738-743.
7. G. Renaud, R. Lazzari, F. Leroy, *Surf. Sci. Rep.* 2009, **64**, 255-380.
8. P. Müller-Muschbaum, *Springer Berlin*, 2008, 17-46.
9. R. Lazzari, *Journal of Applied Crystallography,* 2002, **35**, 406-421.
10. F. Tuinstra, J.L. Koenig, *The Journal of Chemical Physics*, 1970, **53**, 1126-1130.